DETAIL GUIDE FOR CFD ON THE SIMULATION OF BIOGAS COMBUSTION IN BLUFF-BODY MILD BURNER

M.M.Noor[1,2,], Andrew P.Wandel[1] and Talal Yusaf[2,3]

[1]Computational Engineering and Science Research Centre, School of Mechanical and Electrical Engineering, University of Southern Queensland (USQ), Australia
[2]Faculty of Mechanical Engineering, Universiti Malaysia Pahang (UMP), Malaysia
[3]National Centre for Engineering in Agriculture, USQ, Australia
Email: Muhamad.MatNoor@usq.edu.au / muhamad@ump.edu.my

ABSTRACT

Combustion is still the most important process to generate energy. The improvement of combustion efficiency will give high impact to the cost of energy. Beside experimental testing, computational work nowadays becoming more and more important due to lower cost and acceptable accuracy with minimum error. Especially for new develop model, the computational testing using Computational Fluid Dynamics (CFD) software will reduce a lot of trial and error on experimental work. The detail of CFD step by step was focus for this paper for the biogas MILD combustion bluff-body burner. The simulation was carryout using ANSYS 14.5. The ANSYS Modeller was used to model the burner and ANSYS Meshing was used to mesh the model. Finally the Fluent was used to calculate the solution. The post processing was carryout using CFD-Post. The non-premixed combustion with turbulent realizable k-epsilon was used in the simulation and produce MILD combustion in the combustion chamber.

Keywords: combustion, computational fluid dynamics, bluff-body MILD burner, biogas, ANSYS Fluent 14.5

INTRODUCTION

The high and growing demand for energy in today's world has been met about 80% with a fossil fuels supply (IEA, 2009; Maczulak, 2010). Fossil fuel reserve is questionable (Shafie and Topal, 2009) and the use of fossil fuel resulted in the increase of unwanted pollutants emission. This condition requires urgent development of improve pollutants process and new sources of energy other than fossil fuel. Biogas is one of the option since it is renewable and carbon dioxide produce in the combustion process will be use back by the biomass that grown to produce biogas. MILD Combustion is proven to improve the thermal efficiency and reduce NO_x emissions (Wünning, 1991,1996; Katsuki and Hasegawa, 1998; Dally et al., 2002, 2004, 2010; Tsuji et al., 2003; Szego et al.,2003,2009; Cavaliere et al.,, 2004, 2008; Christo and Dally, 2005; Medwell et al., 2007; Colorado et al., 2009; Joannon et al. 2009; Mi et al., 2009,2010; Oryani et al., 2011; Li et al., 2011a,2011b; Noor et al., 2012a, 2012b; Yusaf et al. 2013). This combustion technique is call flameless oxidation (Wünning and Wünning, 1997; Milani and Wünning, 2007), High Temperature Air Combustion (Katsuki and Hasegawa, 1998; Tsuji et al., 2003) and colourless distributed combustion (Arghode and Gupta, 2010a, 2010b, 2011a, 2011b).

CFD is one of the ways to virtually design and run the simulation experiment without the need to physically build the model. The cost of model building and repeat the process until the desired result is very huge. This process can be done by CFD modelling using commercial software and it is very much cheaper compare to physical

model building. CFD has been successful in carried out the simulation on many engineering problem (Baukal et al., 2001 and Davidson, 2002) such as gas turbine (Al-Habbouni et al., 2006 and Duwig et al., 2008), industrial furnace (Hekkens, 2004; Sheng et al.,2004; Yang and Blasiak, 2006; Stefanidis et al., 2006; Chen et al., 2012), boilers (Rahimi et al., 2006; Khoshhal et al., 2009,2010,2011), internal combustion engine (Barths, 2000; Kong and Reitz, 2002; Ghamari and Nasiritosi, 2003, Devi et al., 2004; Ganesan et al., 2004; Ling and Tun, 2006; Siqueura et al., 2006; Noor et al., 2008), flameless combustor (Hasegawa et al., 2002; Porcheron et al., 2005; Donatini et al.,2005,2008; Acon et al., 2007; Mancini and Webber, 2008; Galetti et al., 2008; Mollica et al., 2010; Rebola et al., 2010; Noor et al., 2012c,2012d,2013) and other engineering applications (Dally et al., 1998; Hanjalik, 1999; Fletcher et al., 2000; Yimer et al., 2001; Wandel et al., 2003; Nardo et al., 2009; Ramasamy et al., 2009; Najiha et al., 2012a, 2012b; Lam et al., 2012). The simulation also can be done by using the discretization of the fluid flow equations with Finite Difference Method (FDM) and Taylor expansion and then writing the coding using FORTRAN (William and McCracken, 1972; Press, 1992; Kee et al., 1989; Noor et al., 2012e) or MATLAB (Wandel, 2005, 2011, 2012; Clarke et al., 2010; Hairuddin et al., 2011).

This paper drafts step by step of CFD simulation for the non-premixed MILD combustion furnace with biogas as a fuel. The work use ANSYS workbench with Fluent is the software for solution and post processing to review the result. The simulation starts with design modeller to model the 3D furnace. The meshing of the model used ANSYS meshing and finally the solution use ANSYS Fluent.

GOVERNING EQUATIONS

CFD calculation and mathematical processes are governed by fluid flow governing equations. The equations are series of fluid properties which are mass conservation (continuity equation), density, temperature, species, mass fraction, enthalpy, turbulent kinetic energy (k) and turbulent dissipation rate (ε). For the axisymmetric flow in low Mach number (M < 0.3) (Rehm and Baum, 1978; Majda and Sethian, 1985), the transport equations are:

Mass (the continuity equation)

$$\frac{\partial \rho}{\partial t} + \nabla.\rho U = 0 \quad (1)$$

Momentum

$$\frac{\partial \rho U}{\partial t} + (\nabla.\rho UU) = -\nabla p + \nabla.\tau + \rho g \quad (2)$$

Enthalpy

$$\frac{\partial \rho h}{\partial t} + \nabla.\rho U = \nabla.\lambda_e \nabla T - \nabla.q_{rad} + \nabla.\sum_l \rho h_l(T) D_e \nabla m_l \quad (3)$$

Temperature

$$\rho c_\rho \frac{DT}{Dt} = \nabla.\lambda_e \nabla T - \nabla.\sum_l \rho h_l(T) D_e \nabla m_l - \rho \sum_l \frac{Dm_l}{Dt} h_l(T) \quad (4)$$

Species mass fraction

$$\frac{\partial \rho m_l}{\partial t} + \nabla.\rho U m_l = \nabla.D_e \rho \nabla m_l - R_l \quad (5)$$

The most common turbulent model is k-ε model (Jones and Launder, 1972; Launder and Sharma, 1974). This model was practical for many flows and relatively simple to implement and easy to converge. The equation for turbulent kinetic energy (k) is (6) and turbulent dissipation rate (ε) is (7).

$$\frac{\partial}{\partial t}(\rho k) + \frac{\partial}{\partial x_i}(\rho k u_i) = \frac{\partial}{\partial x_j}\left[(\mu + \frac{\mu_t}{\sigma_k})\frac{\partial k}{\partial x_j}\right] + P_k + P_b - \rho\epsilon - Y_M + S_k \quad (6)$$

$$\frac{\partial}{\partial t}(\rho\epsilon) + \frac{\partial}{\partial x_i}(\rho\epsilon u_i) = \frac{\partial}{\partial x_j}\left[(\mu + \frac{\mu_t}{\sigma_\epsilon})\frac{\partial\epsilon}{\partial x_j}\right] + C_{1\epsilon}\frac{\epsilon}{k}(P_k + C_{3\epsilon}P_b) - \rho C_{2\epsilon}\frac{\epsilon^2}{k} + S_\epsilon \quad (7)$$

where turbulent viscosity, $\mu_t = \rho C_\mu \frac{k^2}{\epsilon}$, production of k, $P_k = -\overline{\rho u_i' u_j'}\frac{\partial u_j}{\partial x_i}$, effect of buoyancy, $P_b = \beta g_i \frac{\mu_t}{Pr_t}\frac{\partial T}{\partial x_i}$ and $\beta = -\frac{1}{\rho}(\frac{\partial\rho}{\partial T})_p$. In the effect of buoyancy, g_i is the component of the gravitational vector in the i*th* direction and Pr is turbulent Prandtl number. Pr is 0.85 for the standard and realizable k- ε model. Other model constants are $C_{1\epsilon}, C_{2\epsilon}, C_{3\epsilon}, C_\mu, \sigma_k$ and σ_ϵ. The common fluid flow problem can be solved in one dimension, two dimensions or three dimensions with parabolic, elliptic or hyperbolic equations.

DESIGN MODELLER

The design modeller software in the ANSYS workbench was utilised to draw the MILD furnace as Figure 1. This task of drawing also can be done using other commercial computer aided drawing software like AutoCAD, Solidwork, Unigraphic and many others. In order to speed up the solution, the model must be small and simple, but meet the required model drawing and shape. This is due to the smaller the model, the lesser the meshing node and element to be calculated later. The mesh grid quantity will directly impact to the solution duration. If the model were symmetrical, the model can be cut into half (Figure 1(b)) or even quarter (Figure 1(c)). The geometry of the model includes volumes, surface, edges and vertices. All of these items can be selected for the meshing techniques.

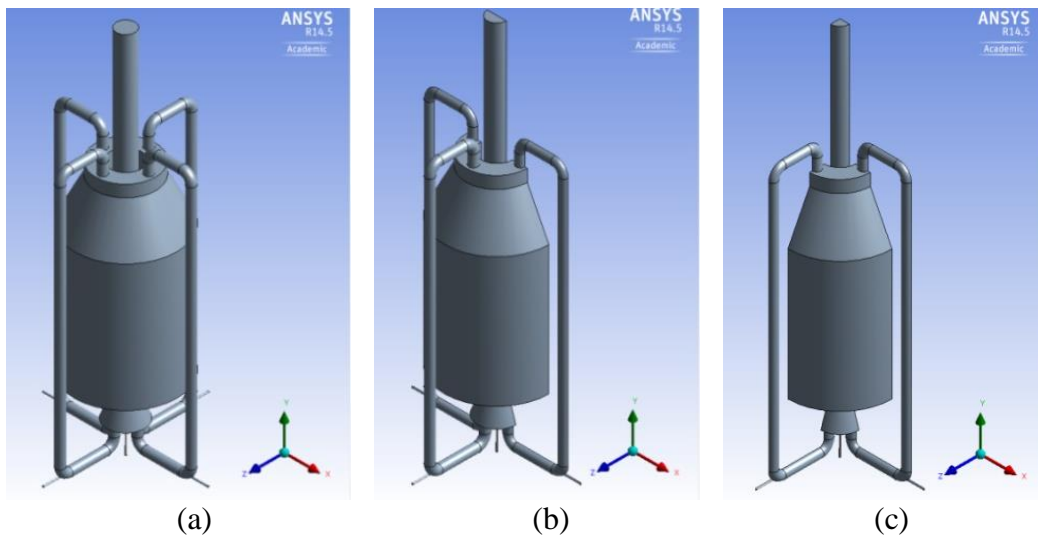(a)   (b)   (c)

Figure 1. Design modeller for the MILD furnace (a) full model, (b) half model axisymmetric at XYPlane (c) quarter model axisymmetric at XYPlane and YZPlane

MESHING

The most critical part of the CFD process is model meshing. The quality of meshing will be determined the technique of the meshing. Meshing will create grid of cells or elements which all the desired fluid flow equations to be solved. The size of the grid will give significant impact to the computational time or Central Processing Unit (CPU) time which directly involves cost of the simulations. The grid also will give significant effect for the convergence speed and the solution accuracy. Industrial CFD problems normally consist of large numerical grids cells (Peters, 2004).

Inflation is very important for the new wall area or boundary layer mesh. Figure 2 show the plain meshing without inflation and detail sizing at some important area. Figure 3 show the meshing with inflation and nozzle area with body of influence and edge sizing technique. The skill and quality of meshing process is required many practice and try and error since it's a very complex process. The practice can be done following the ANSYS meshing tutorial that available in their website. Meshing process must be start at coarse mesh (Table 1) and check the quality at the statistics (Table 2). The required quality to be check is skewness and aspect ratio on mesh metric and smoothness (change in cell size). The maximum skewness must be below 0.98 or the solution will be easy to become divergence error and will not converge as desired. Some model and setting may be having different limit range from 0.85 to 0.98. The overall range of skewness is from zero to one where the best is zero and worst is one. The skewness value is calculated based on equilateral or equiangular shape. For example the skewness for equilateral is the ratio of the optimal cell size minus actual cell size divided by optimal cell. For this case, coarse mesh giving maximum skewness of 0.9817 and it is higher than allowable value. The medium or fine mesh is needed to ensure the skewness is below 0.98. When the meshing use fine relevance centre and other setting as final setting in Table 1, the maximum skewness is lower to 0.8458 and it is below 0.85 which the tightest limit.

Table 1. Mesh sizing setting parameters

Sizing parameters	Beginning setting	Final setting
Advance size Function	Proximity and Curvature	Proximity and Curvature
Relevance centre	Coarse	Fine
Initial Size seed	Active assembly	Active assembly
Smoothing	Low	High
Transition	Fast	Slow
Span Angle Centre	Coarse	Fine
Curvature Normal Angle	Default (70.3950^{o})	Default (18.0^{o})
Proximity Min Size	0.5	0.5
Num Cells Across Gap	Default (3)	Default (3)
Min Size	Default (1.21770 mm)	Default (0.356650 mm)
Proximity Min Size	Default (1.21770 mm)	Default (0.356650 mm)
Max face Size	Default (121.770 mm)	Default (35.6650 mm)
Max Size	Default (243.540 mm)	Default (71.3290 mm)
Growth Rate	Default (1.850)	Default (1.20)
Minimum	1.0 mm	1.2 mm

The aspect ratio is calculated by dividing the longest edge length to shortest edge. The best aspect ratio is 1.0 means the cell is nicely square or equal edge length of any shape. The cell shapes was triangle and quadrilateral for 2D problem and tetrahedron, hexahedron, pyramid wedges and polyhedron for 3D problem. The smoothness or the change of the cell size must be gradually and must not be more than 20% change from cell to the next cell. If there are cells that jump in size, the smoothness will be very bad and the solution will be hard to converge. The node and element quantity is very critical since it will affect the final result and the computational time which is also computational cost. The higher the meshing element, will give the better final result but the longer computational time to complete the simulation. At this point, the acceptable mesh quality will be the best solution for both acceptable final result and computational time. The dynamic mesh is not applicable for this problem.

Table 2. Statistic on nodes, elements and mesh metric for skewness and aspect ratio

Item	Beginning setting	Final setting
Nodes	75,460	244,650
Elements	197,747	700,161
Mesh Metric	Skewness	Skewness
Min	2.44839909654182E-04	8.11678841107222E-05
Max	0.981734647631257	0.8457743626017
Average	0.357655823424707	0.227029865966053
Standard Deviation	0.164923824872058	0.127163635668632
Mesh Metric	Aspect Ratio	Aspect Ratio
Min	1.165	1.053
Max	649.49	209.09
Average	15.9406852407369	9.20230909805037
Standard Deviation	34.3018343757542	15.5276176469768

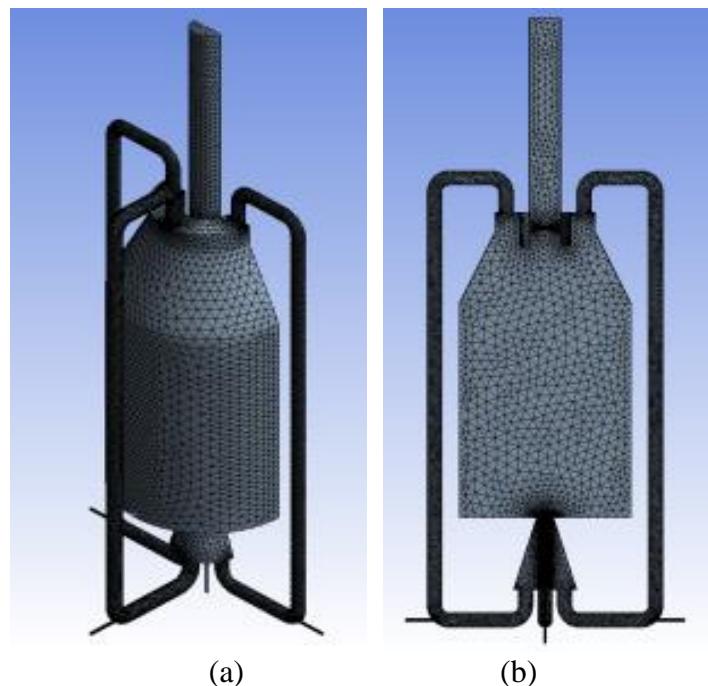(a)   (b)

Figure 2. Model after meshing (a) 2D view (b) 3D view

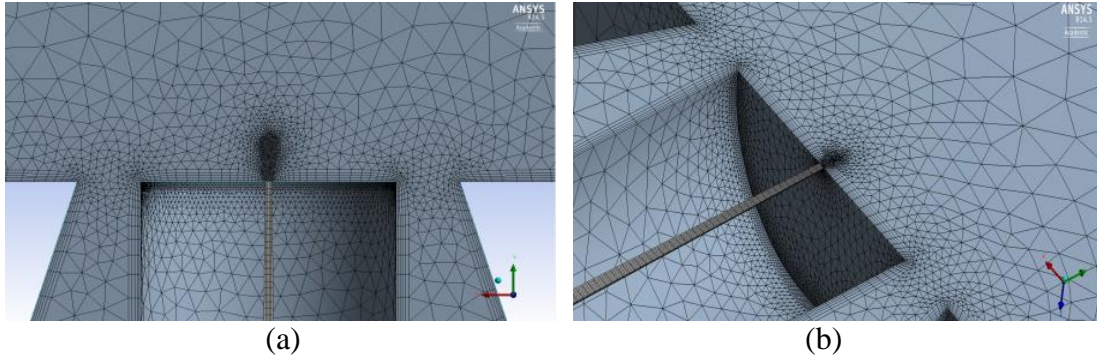<div align="center">(a)   (b)</div>

Figure 3. Fine mesh at fuel and air nozzle inlet (a) 2D view (c) 3D view

The setup for the near wall needs to use the inflation. In this case the inflation setting is as shown in Table 3. The stair stepping is use to avoid the collision. If the collisions still happen then change the setting to layer compression. Numbers of layer is 5 with growth rate is 20% and maximum thickness is 2.0 mm.

<div align="center">Table 3. Inflation setting parameters</div>

Item	Setting
Use Automatic inflation	Program controlled
Inflation Option	Total thickness
Inflation Algorithm	Pre
View Advanced Option	Yes
Collision Avoidance	Stair stepping
Growth Rate Type	Geometric
Use Post Smoothing	Yes
Number of Layers	5
Growth Rate	1.2
Maximum Thickness	2. mm
Gap Factory	0.5
Maximum Height Over Base	1
Maximum Angle	140.0
Fillet Ratio	1
Smoothing Iterations	5

For the nozzle inlet, the size is very small and need special meshing treatment like sweep method, face sizing and edge sizing. Number of division is selected for the edge sizing technique. In the area of fuel jet mix with air jet, need super fine mesh and this can be done by using the body sizing meshing technique. There are 3 types of body sizing which are element size, sphere of influence and body of influence. For the body of influence, the scope geometry is the whole body selection and for the body if influence, add frozen body need to be draw in the design modeller as Figure 4(a). The mesh result for the body of influence as shown in Figure 4(b). The body of influence meshing is very sensitive and if need to repeat the process, then remove the frozen body and draw again and re-do the process.

We can use sphere of influence, but it will give higher number of nodes and element and make more computational time to run the simulation. The sphere centre
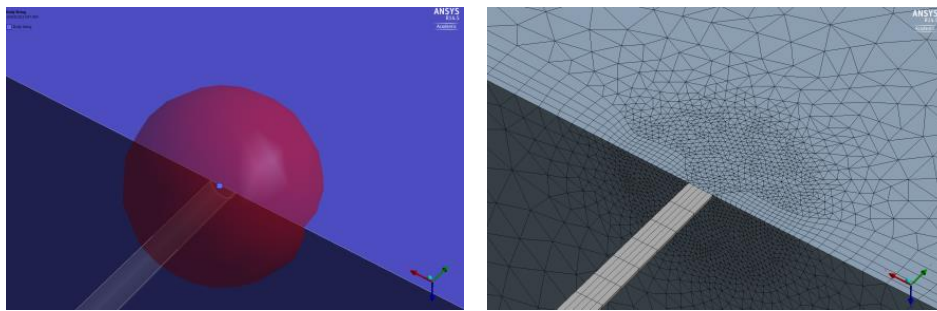
need to be selected with normally use XYPlane and the sphere radius need to be set as Figure 5(a). The mesh result for the body of influence as shown in Figure 5(b).
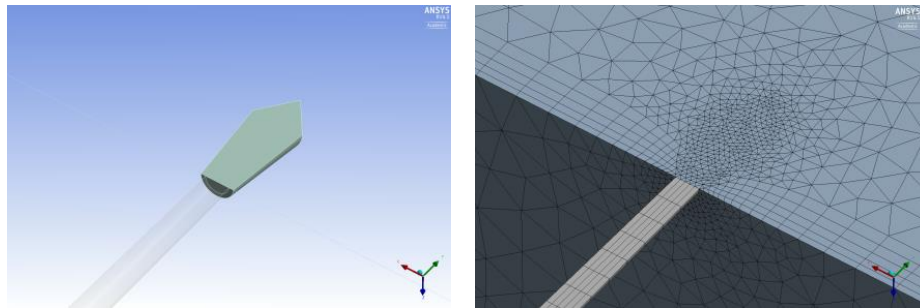
(a)   (b)

Figure 4. Body sizing meshing for body of influence (a) geometry (b) meshing

(a)   (b)

Figure 5. Body sizing meshing for sphere of influence (a) geometry (b) meshing

SOLUTION SETUP

The setup screen is required the setting of the option on single or double precision. If double precision used, the solution will be slower and it's not necessary for many cases. The processing option is the setting of single or parallel processor on local machine. For one license, maximum of four parallel computer processors can be used. This is applicable to the multicore processor computers and not for single processor computer. To increase the parallel processor to more than four, second license is needed. Figure 6 show the setup screen.
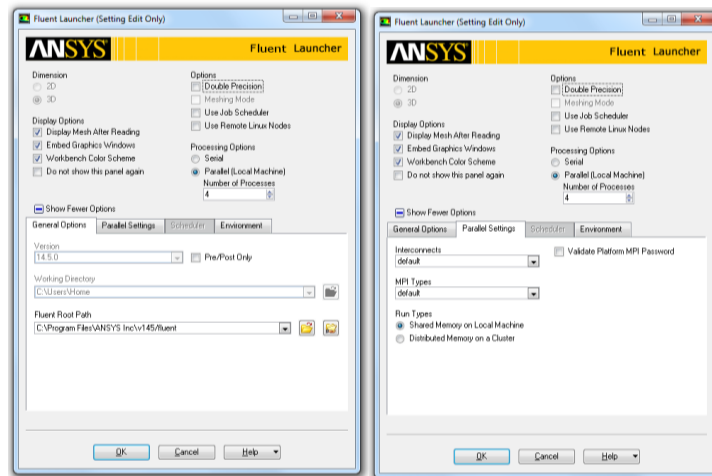
(a)   (b)

Figure 6. Fluent launcher CFD setup (a) general option (b) parallel setting

7

Ensure the unit for the model is correctly setup in general setting. Record the domain extend measurement since it may need when the setting of plane cutting to view the result. Check the report quality to ensure the mesh quality is acceptable. An orthogonal qualities range is from 0 to 1, where the lower value means lower quality. This case the minimum orthogonal quality is 0.129378. The solver setting is depending on the case for type of solver in between pressure-based and density based. The solver selection is also need for velocity formulation setting between absolute and relative and for time between steady or transient solution. This case use pressure-based, absolute velocity and steady solver. The gravitational accelerations setting are on Y direction with -9.81 m/s^2.

The setting for models (Appendix A) is the most important since these parameters setting is related to the simulations condition including energy, radiation, turbulent viscous and species. The energy equation must be on since the case having the temperature change in the combustion process. The turbulent viscous model selection is realizable k-epsilon with standard wall function as near wall treatment. The discrete ordinate (DO) is chosen for the radiation and non-premixed is for species. Some of the setting will be explained further later in next section. PDF mixture is used for the material and the species count is depending on the model setting (Table 4 and Figure 7). The pressure is set at 101.325 kPa and Fuel Stream Rich Flammability Limit (FSRFL) is set as Table 4 for model setting under the setting of for non-premixed combustion.

Table 4. PDF table creation for model setting parameters for Fuel Stream Rich Flammability Limit (FSRFL)

Oxygen level (%)	Stoichiometric FSRFL	Stoichiometric FSRFL + 10%	Species
1	0.015	0.0165	8
3	0.024	0.0264	8
5	0.038	0.0418	8
7	0.052	0.0572	9
9	0.066	0.0726	11
11	0.080	0.088	11
13	0.092	0.1012	13
15	0.105	0.1155	13
17	0.117	0.1287	13
19	0.130	0.1430	14
21	0.142	0.1562	16
23	0.155	0.1705	17
25	0.167	0.1837	18
27	0.178	0.1958	18

The PDF table creation boundary condition for the fuel and oxidant was set as shown in Table 5. The biogas fuel was created by the mixing of methane (60%) and carbon dioxide (40%) on molar basis. This biogas mixing ratio was also used by other researchers (Pomeroy, 2008; Colorado et al., 2010; Scholz and Ellner, 2011; Salunkhe et al., 2012; Noor et al., 2012a; Keramiotis and Founti, 2013) in their biogas researched. For the oxidant, the mixing of nitrogen (79%) and oxygen (21%) was use as the normal

combustion air configuration. The fuel and oxidant temperature was set at 300 K. The other table parameters for the PDF creation were set as shown in Table 6.
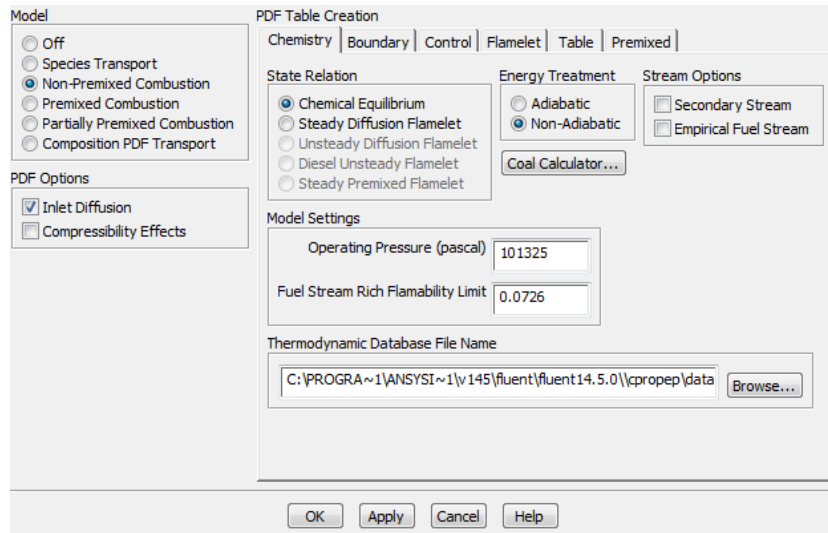

Figure 7. Model species window for the selection of non-premixed model with the chemistry state relation and fuel stream rich flamibility limit setting

Table 5. PDF table creation for Boundary condition parameters

Species	Fuel	Oxidant
CH_4	0.60	0
H_2	0	0
N_2	0	0.79
O_2	0	0.21
CO_2	0.40	0

Table 6. PDF table creation for parameters for PDF table calculation

Item	Setting
Initial Number of Grid Point	15
Maximum Number of Grid Point	200
Maximum Change in Value Ratio	0.25
Maximum Change in Slope Ratio	0.25
Maximum Number of Species	20
Minimum Temperature	300

Then after this setting is confirm, click inlet diffusion at PDF option and automated grid refinement. Finally calculate PDF table and Fluent will calculate and display the result as how many species (material) created and can be check under the material in the next steps. Table PDF can be check by display table PDF and choose the figure type as 2D or 3D and what parameters to display (default is 3D Figure: mean temperature, mean mixture fraction and scaled variance) (Figure 8).

The boundary condition is the setting for the inlet, wall and outlet. In this case there are 4 air inlets, 1 fuel inlet, 1 exhaust and 1 wall for the whole chamber. For the air inlet and fuel inlet, the momentum setting for the velocity specification method is using

the component method. The Cartesian coordinate system was use in line with the model coordinate system. The velocity for air inlet was in the x and z direction as shown in Figure 9. Under the thermal setting, the temperatures was set to 300 K and for the species setting, mean mixture fraction was set to zero. The velocity for the fuel inlet was in Y direction and thermal (temperature) setting is 300 K but the mean mixture fraction was set to unity. Turbulence specification method was intensity and hydraulic diameter which turbulence intensity was set to 5% and hydraulic diameter is 10 mm as per model measurement. The velocity for the air and fuel inlet is in unit m/s is one of the main parameters that need to change depending on air fuel ratio of the biogas and oxidant (Noor et al., 2012b, 2012f). The wall setting is stationary wall and no slip shear condition with thermal heat flux 0 w/m^2 and internal emissivity of 1.
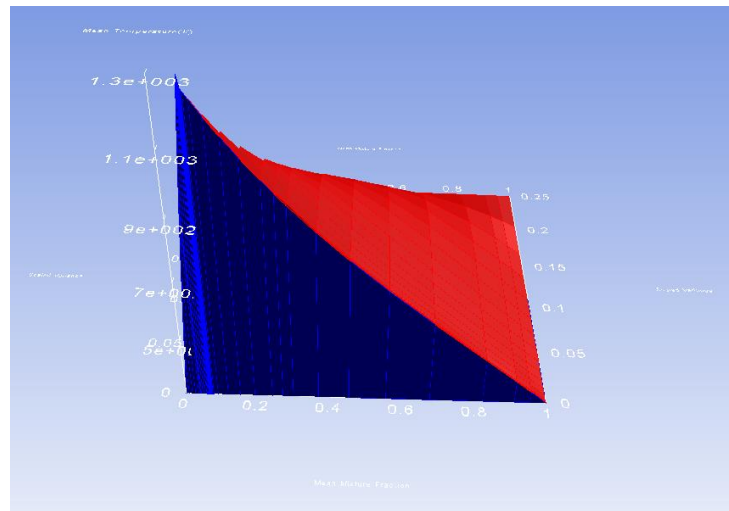

Figure 8. Display PDF table for mean temperature, mean mixture fraction and scaled variance

Figure 9. Boundary condition for the air inlet, fuel inlet and exhaust

SOLUTION

The solution of the simulation involved chemical reactions since it is non-premixed combustion process, heat transfer, turbulent flows and species transport. The simulation was using Reynolds-Averaged Navier–Stokes (RANS) equations solve together with a realizable k-ε turbulence model (Shih et al., 1995) [that developed based on standard k-ε turbulence model (Launder and Spalding, 1974)] are solved using commercial CFD software ANSYS Fluent 14.5 (Fluent, 2012). The discrete ordinate (DO) radiation model (Fiveland, 1982, 1984; Chui and Raithby, 1993; Li et al., 2002) and absorption coefficient of weighted sum of gray gas (WSGGM) model (Hottel and Sarofim, 1967; Smith et al., 1982; Soufiani and Djavdan, 1994) is used in this work. The selection of WSGGM model is suitable for this work due to giving a reasonable compromise between oversimplified gray gas assumption and complete model accounting for the entire spectral variations of radiation properties (Yeoh and Yuen, 2009).

The solution method setting (Table 7) shows the original setting and new setting for the case. For the beginning of the solution, start the calculation with original and after stable then change the setting to new setting and run the calculation until it converges. The couple method use for the pressure-velocity coupling scheme with least square cell based gradient and presto for pressure. For the momentum, turbulent kinetic energy, turbulent dissipation rate, pollutant no, energy, discrete ordinates, mean mixture fraction, and mixture fraction variance, the second order upwind is suitable when the solution to run in the final stage.

Table 7. Solution method parameter setting

Parameters	Original setting	New setting
Pressure-Velocity Coupling	SIMPLE	Couple
Gradient	Green-Gauss Cell Based	Least Squares Cell Based
Pressure	Standard	PRESTO!
Momentum	First Order Upwind	Second Order Upwind
Turbulent Kinetic Energy	First Order Upwind	Second Order Upwind
Turbulent Dissipation Rate	First Order Upwind	Second Order Upwind
Pollutant no	First Order Upwind	Second Order Upwind
Energy	First Order Upwind	Second Order Upwind
Discrete Ordinates	First Order Upwind	Second Order Upwind
Mean Mixture Fraction	First Order Upwind	Second Order Upwind
Mixture Fraction Variance	First Order Upwind	Second Order Upwind

The solution control for flow Courant number, Explicit Relaxation Factor (ERF) and Under-Relaxation factor (URF) shows in table 8. For the beginning of the simulation, the calculations need to be run with the original value of parameters setting and evaluate the result. In many complex cases with the simulation include chemical reaction such as combustion, the original setting will give the divergence error and need more attention. If the solution is diverge, the flow courant number and relaxation factor need to change depending on the error of divergence. In this case, the error is enthalpy and the new setting is reduce the flow courant number from 200 to 50 and reduce the relaxation factor for momentum, pressure and density as Table 8. The reduction of relaxation factor will slow down the convergence process.

Table 8. Solution control parameters for flow courant number, explicit relaxation factor and under-relaxation factor

Parameters	Original value	New value
Flow Courant Number	200	50
ERF: Momentum	0.75	0.3
ERF: Pressure	0.75	0.45
URF: Density	1.0	0.3
URF: Body Force	1.0	1.0
URF: Turbulent Kinetic Energy	0.8	0.8
URF: Turbulent Dissipation Rate	0.8	0.8
URF: Turbulent Viscosity	1.0	1.0
URF: Pollutant NO	0.9	0.9
URF: Energy	1.0	1.0
URF: Temperature	1.0	1.0
URF: Discrete Ordinates	1.0	1.0
URF: Mean Mixture Fraction	1.0	1.0
URF: Mixture Fraction Variance	0.9	0.9

For the monitoring of the calculation process, the residual of convergence criteria use is absolute and the criteria is set at 0.000001 to ensure the convergence process is smooth (Figure 10). The initialize processes use the hybrid and the setting is automatically pre-set by the software. Then the patch is depending on the model need. In this case the patch is use for Y velocity, then need to force the flow downward (negative Y) for exhaust gas recirculation (EGR) pipe. The patch for Y velocity is -10 m/s. The second patch is for temperature 350 K. This is about 50 K above the room temperature.
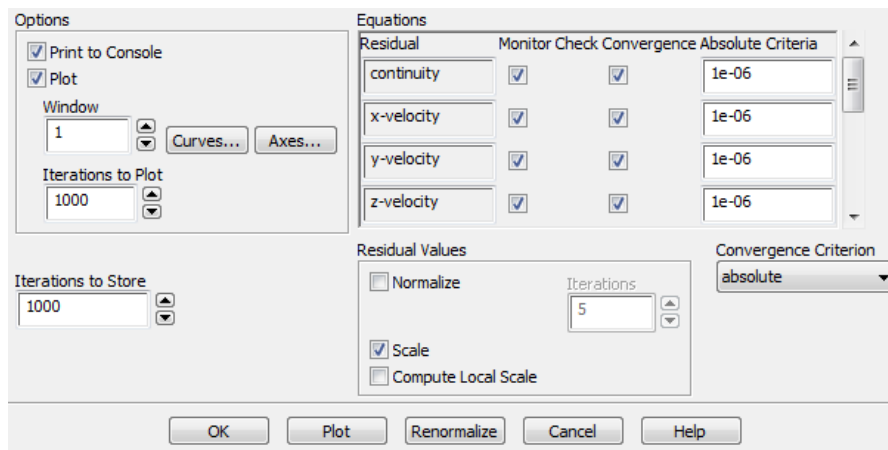

Figure 10. Residual monitor for convergence criteria

For calculation activities, we use execute commands (Table 9) to generate a series of image step by step and combine the image by using image sequence in the Apple QuickTime or other software and those image will become a movie of flame from start to end of the iterations. The file name in this case is B17AN14D76FN10x21A15Pic-%i.tif and *.tif file will be save for every 1 iteration.

The iteration pictures that generate by that command will be saving as running number of 0001 to 9999 at the end of the filename (B17AN14D76FN10x21A15Pic-0001.tif). The display during the calculation will be shown as Figure 11, where residual monitoring is on window 1 (Figure 11(a)) and xyplane contour surface at window 2 (Figure 11(b)).

Table 9. Execute commands under calculation activities

Numbering	Iterations		Command
Command-1	1	Iteration	disp set-window 2
Command-2	1	Iteration	disp set contour surface xyplane
Command-3	1	Iteration	disp contour temperature
Command-4	1	Iteration	disp view restore-view front
Command-5	1	Iteration	disp hc B17AN14D76FN1Ox21A15Pic-%i.tif

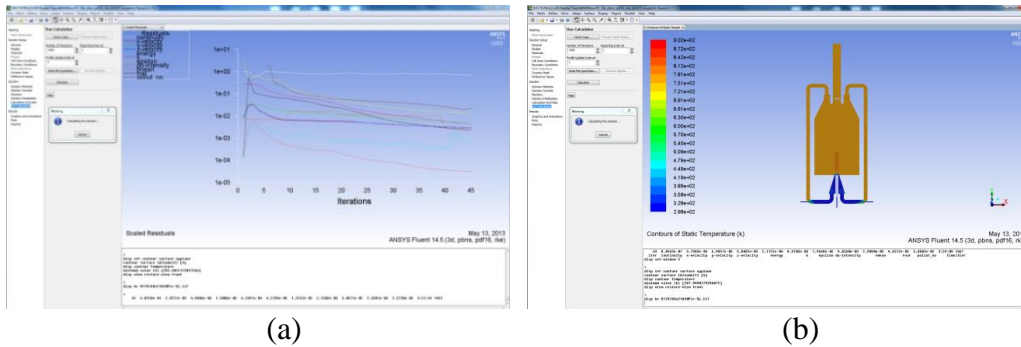(a)   (b)

Figure 11. Monitoring window during calculation (a) window 1 (b) window 2

Before the calculation process start, check case need to carryout to ensure no error and the model are ready to be simulated. The check case is checking the mesh, models, boundaries and cell zone, materials and solver. In this example, the calculation was setup up at 4500 iterations as Figure 12.
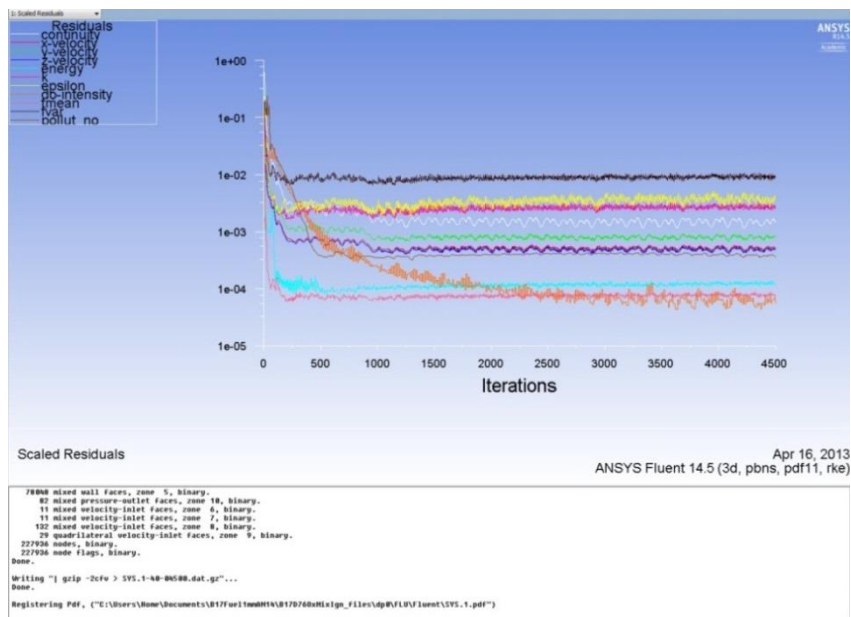

Figure 12. Converge solution

13

The calculation was converging and result was satisfied with non-premixed combustion occurred and MILD achieve as expected. To achieve the convergence, many trial and errors were done especially on Explicit Relaxation Factor (ERF) and Under-Relaxation factor (URF). Figure 13 shows one of the examples of common error which is primitive error at node 1: floating point exception (divergence detected in AMG solver: enthalpy or some time the error of divergence detected in AMG solver: epsilon). To solve this error flow courant number and three relaxations factor is tested and finally reach the optimum values.

The convergence of the solution is very important to ensure the end result of the simulation is correct and accurate. The relaxation method may be used to speed up or delay the solution by using the relaxation factor. The relaxation factor (λ) can be seen in below equation.

$$\phi_{i,j,k}^{new} = \lambda\phi_{i,j,k}^{p} + (1-\lambda)\phi_{i,j,k}^{p-1} \tag{7}$$

where λ is between 1-2 and $\phi_{i,j,k}^{p}$ is the value from the present iteration and $\phi_{i,j,k}^{p-1}$ is the value from the past iteration. The convergence can be monitored by the residual (Figure 12 and 13). If λ is less than 1.0, this is under-relaxation and will slow down the convergence and it becoming more time for the simulation. Anyway under-relaxation will increase the calculation stability and reduce the divergence possibility. If λ is equal to 1.0, that means there is no relaxation applied. If λ is more than 1.0, that is call over-relaxation. Over-relaxation will speed up the convergence but at the same time will reduce the calculation stability and giving high possibility for the solution to diverge. The most sensitive relaxation factor for the combustion simulation is energy, temperature, radiation (discrete ordinates) and mean mixture fraction. These items normally will use 1.0 as relaxation factors. For under-relaxation factor (Table 8), its advice to use high relaxation factor (near to or 1.0) since if it too low, the convergence is too slow and may not be converge even its look like converge. The default relaxation factor is the propose factor by the solver and if the solution is still diverge, explicit relaxation factor (momentum and pressure) can be reduce to slow down the convergence (Table 8).
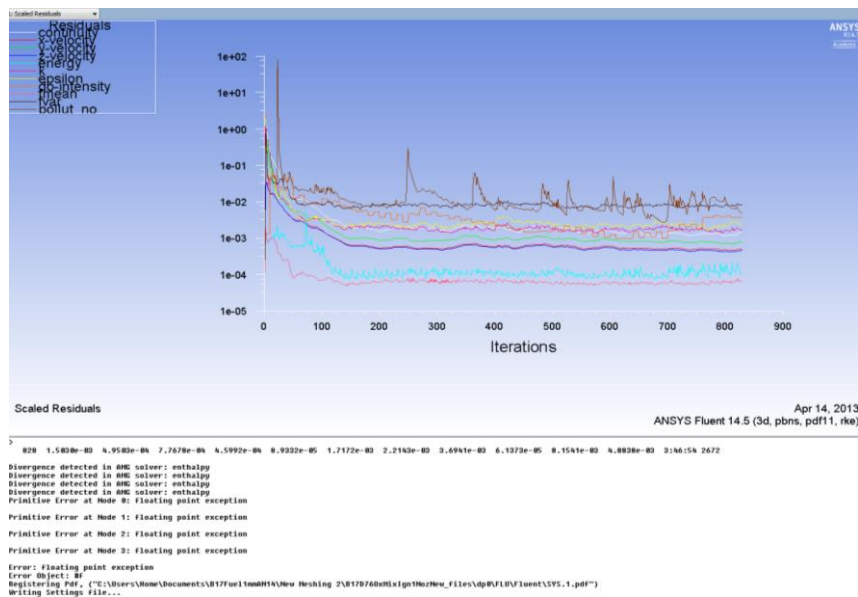

Figure 13. Error on divergence detected in AMG solver: enthalpy

The convergence of the simulation is considered achieve if the residual is stable or no more change from iteration to next iteration (Figure 12). If the residual already achieve lower limit set by the residual monitor but still show reducing trend, the solution may not be converge until the residual is stable. The lower limit for the residual is normally set at 1.0×10^{-6}. For some cases the lower limit is set at between 1.0×10^{-3} to 1.0×10^{-6}.

RESULTS

The result of the simulation can be presented in graphical view or numeral as flow fields through export function (File → Export → Solution data). The options for the graphical result were contours plots, vector plots, iso-surfaces plots or animations. The most common used was contour plots and vector plots. The result shown in Figure 14 is from contours on the graphics. The option was set as filled, node values, global range and the contour on Figure 14(a) is 2D view of the velocity magnitude from the XY plane. The plane was set at the surface option and then select plane. The plane surface setting to create xyplane is shown in Figure 15. The temperature contour result (Figure 14(b)) was in two plane on 2D view which are xyplane and yzplane created same technique as xyplane. The temperature contour is homogeneous throughout the combustion chamber shown that MILD combustion was achieved.
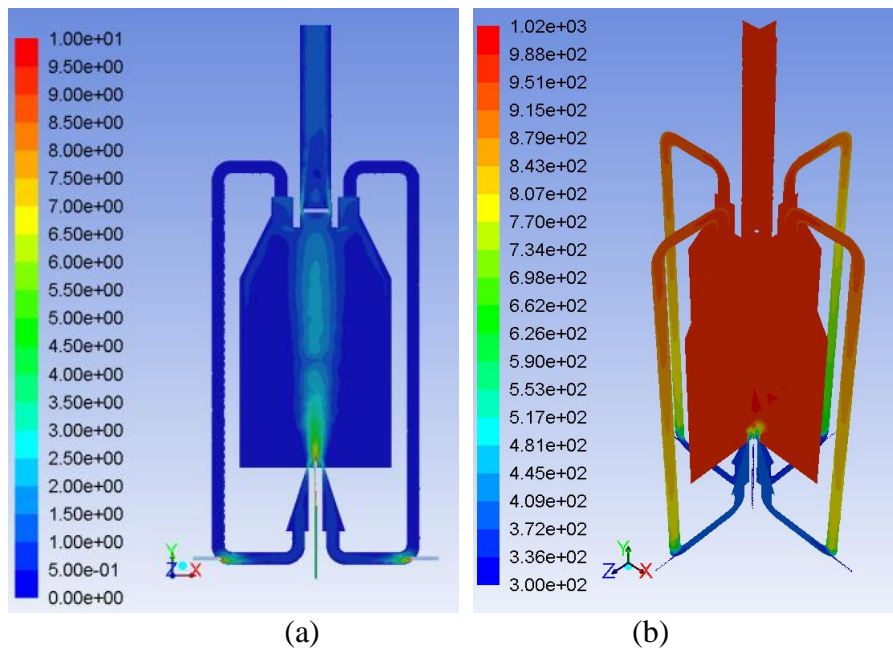

Figure 14. Result (a) 2D view for velocity magnitude (b) 3D view for temperature distribution

If we use the result from ANSYS workbench component system (ANSYS Results) for the post processing, the flow streamline (Figure 16) and the wall contour (Figure 17) can be develop and analyse. Figure 16(a) shows the 3D velocity streamline for all domains with 25 point sampling equally spaced start from the fuel inlet with forward and backward direction. Figure 16(b) with the same setting but start from the air inlet 1. The streamline is more than the fuel inlet since the volume of air inlet is higher than the fuel inlet. For both streamline, the flow through the EGR pipe is

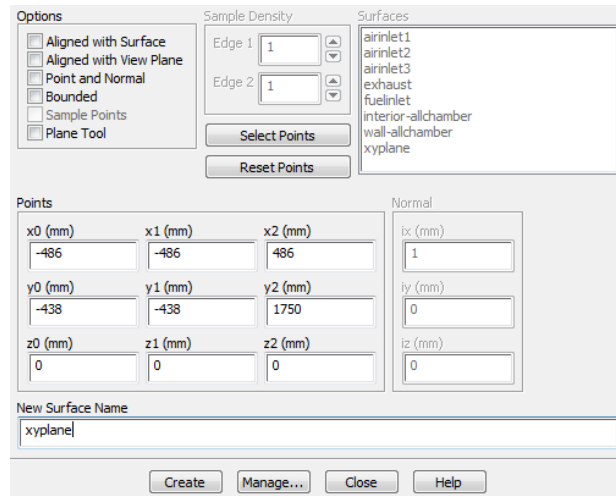downward can be seen clearly. Some exhaust flow out from the exhaust outlet can be observed in Figure 16(b).

Figure 15. 2D xyplane setting the view contour result

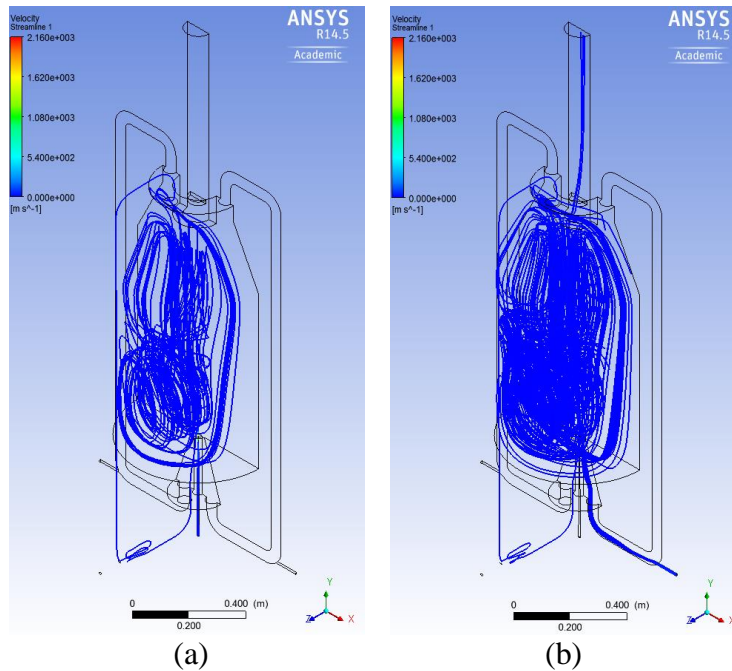|	
(a)	(b)

Figure 16. Result for velocity streamline (a) start from fuel inlet (b) start from air inlet

The contour result for the wall temperature can be plotted. The wall temperature is at the range of 983 to 1012 K and it's homogenously distributed. The temperature for the EGR pipe wall is reducing from 983 to 1012 K at the top (early of EGR) and reduces to the range of 537 to 636 K before mix with fresh air at 300 K. When the hot flue gas (EGR) mixed with fresh air, the temperature of the mixing further down to the range of 418 to 537 K before entering back to the combustion chamber. This condition can be seen as fresh air been preheated by the EGR from 300 K to the range of 418 to

537 K. The oxygen content in the fresh air also been diluted and this preheating and dilution of the oxidant makes the furnace achieve MILD combustion regime.
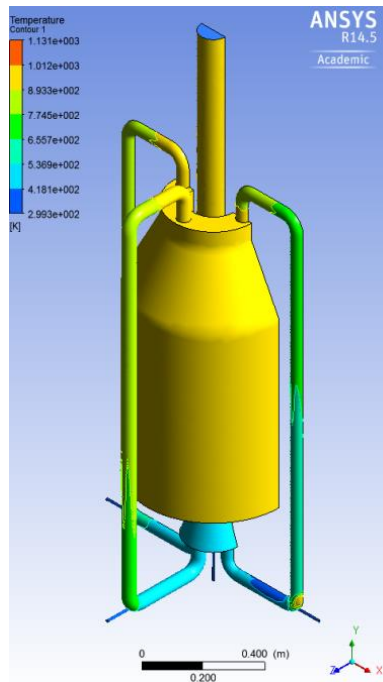

Figure 17. Result for temperature contour on the furnace wall

CONCLUSION

The simulation for the non-premixed MILD combustion with biogas as fuel was successful by using ANSYS Fluent 14.5. The step by step guide and setting was discussed. Below conclusion can be drawn.

   i.   The most important and critical step in CFD work is meshing. The quality of meshing is giving the highest influence of the calculations whether it will converge and produce good result or diverge and giving error result.

  ii.   The models setting (Appendix A) at the beginning of the solution steps must be correctly selected according to the problem to be solved.

 iii.   The parameters setting to create PDF table will give the impact on species and combustion reactions.

 iv.   The meshing quality can be checked by the skewness and aspect ratio on mesh metric and smoothness (change in cell size). The maximum skewness must not exceed 0.98 or in cases of modelling, it must not exceed 0.85

  v.   Meshing technique must be good to ensure the detail mesh at critical and important fluid flow area can be nicely solved.

 vi.   The selection of the solution method and solution control must be suitable for the model and equation to be solved.

 vii.   The divergence of the solution is commonly can be solved by changing the explicit and under relaxation factors. The advisable changing rate is about 10% each time to carry out new simulations.

viii.   The residual monitoring is very useful tools to monitor the iteration steps whether it converge or diverge. The residual will be converge when the value is stable and not further down.

ix. The solution movie can be done by saving step by step pictures (contour temperature) that capture for each iteration.

x. The result of the contour temperature can be plot from the ANSYS Fluent or the flow streamline can be plotted from the ANSYS Result from the workbench under the component systems.

xi. The computer with multicore processor can be used up to 4 numbers of processor for each single license in parallel run settings.

xii. The fresh air been preheated by the EGR from 300 K to the range of 418 to 537 K. and the oxygen been diluted resulted the burner achieved MILD combustion condition as expected.

ACKNOWLEDGMENTS

REFERENCES

Acon, C. H. J., Sala, J. M. and Blanco, J. M. 2007, Investigation on the design and optimization of a low NO_x-CO Emission burner both experimentally and through CFD simulations, Energy and Fuels 21(1), 42-58

Al-Halbouni, A., Giese, A., Flamme, M. and Goerner, K. 2006, Applied modelling for bio- and lean gas fired micro gas turbines, International Journal of Progress in Computational Fluid Dynamics 6(4/5), 235-240

Arghode, V.K. and Gupta, A.K. 2010a. Effect of flow field for colourless distributed combustion (CDC) for gas turbine combustion, Applied Energy, 87(5) 1631-1640

Arghode, V.K. and Gupta, A.K. 2010b. Investigation of distributed combustion for gas turbine application: forward flow configuration. ASME Power Conference, Chicago, Illinois

Arghode, V.K. and Gupta, A.K. 2011a. Investigation of forward flow distributed combustion for gas turbine application. Applied Energy, 88: 29-40

Arghode, V.K. and Gupta, A.K. 2011b. Development of high intensity CDC combustor for gas turbine engine, Applied Energy, 88, 963-973

Barths, H., Hasse, C. and Peters, N. 2000 Computational fluid dynamics modelling of non-premixed combustion in direct injection diesel engines, International Journal of Engine Research; 1: 249

Baukal, C. E., Gershtein, V. Y. and Li, X. 2001 Computational fluid dynamics in industrial combustion, CRC Press.

Cavaliere, A. and de Joannon, M. 2004. MILD combustion, Progress in Energy and Combustion Science, 30: 329-366

Cavaliere, A., de Joannon, M. and Ragucci, R. 2008 Highly preheated lean combustion, In: Lean combustion: technology and control. Oxford, UK, Elsevier, 55-94

Chen, L., Yong, S.Z. and Ghoniem, A. F. 2012, Oxy-fuel combustion of pulverized coal: characterization, fundamentals, stabilization and CFD modelling, Progress in Energy and Combustion Science 38, 156-214.

Christo, F.C. and Dally, B.B. 2005. Modelling turbulent reacting jets issuing into a hot and diluted coflow, Combustion and Flame, 142(1-2): 117-129.

Chui, E.H. and Raithby, G.D. 1993. Computation of radiant heat transfer on a non-orthogonal mesh using the finite-volume method, Numerical Heat Transfer B 23 (3):269-288

Clarke, J., Wandel, A. P. and Mastorakos, E. 2010, Analysis of data to develop models for spray combustion, Southern Region Engineering Conference, Engineers Australia, Toowoomba, Australia. Paper ID: SREC2010-F2-1.

Colorado, A.F., Herrera, B.A. and Amell, A.A. 2010. Performance of a flameless combustion furnace using biogas and natural gas, Bioresource Technology, 101(7):2443-2449

Colorado, A.F., Medwell, P.R. and Dally, B.B. 2009. LCV fuels emissions of turbulent non-premixed jet flames under MILD combustion conditions. Proceedings of the Australian Combustion Symposium, 2-4 Dec, Uni. of Queensland, Australia,

Dally, B.B, Riesmeier, E. and Peters, N. 2004. Effect of fuel mixture on MILD combustion, Combustion and Flame, 137(4): 418-431.

Dally, B.B., Fletcher, D.F. and Masri, A.R. 1998 Flow and mixing Fields of turbulent bluff-body jets and flames, Combustion Theory and Modelling 2, 193-219

Dally, B.B., Karpetis, A.N. and Barlow, R.S. 2002. Structure of turbulent non-premixed jet flames in a diluted hot coflow, Proceedings of the Combustion Institute, 29(1): 1147-1154.

Dally, B.B., Shim, S.H., Craig, R.A., Ashman, P.J. and Szego, G.G. 2010. On the burning of sawdust in a MILD combustion furnace, Energy Fuels, 24: 3462-3470

Davidson, D.L. 2002 The role of computational fluid dynamics in process industries, The Bridge 32(4), 9-14.

Devi, R., Saxena, P., Walter, B., Record, B. and Rajendran, V. 2004, Pressure reduction in intake system of a turbocharged-intercooled di DI diesel engine using CFD methodology, SAE Technical Paper 2004-01-1874.

Donatini, F., Schiavetti, M., Gigliucci, G., Gheri, P., Monticelli, M., Mangione, R., Paulozza, A. and Riccardi, J. 2005, CFD simulation and experimental tests on a natural gas/hydrogen mixture-fired flameless combustor, ECCOMAS Thematic Conference on Computational Combustion, Lisbon, Portugal

Donatini, F., Schiavetti, M., Gigliucci, G., Gheri, P., Monticelli, M., Mangione, R., Paulozza, A. and Riccardi, J. 2008, CFD simulation and experimental tests on a natural gas/hydrogen mixture-fired flameless combustor, 8th European Conference on Industrial Furnaces and Boilers, Vilamoura, Portugal

Duwig, C., Stankovic, D., Fuchs, L., Li, G. and Gutmark, E. 2008 Experimental and numerical study of flameless combustion in a model gas turbine combustor, Combustion Science and Technology, 180(2): 279-295.

Fiveland, W. A. 1982, A Discrete-ordinates Method for predicting radiative heat transfer in axissym-metric enclosures, ASME. Paper No. 82-HT-20

Fiveland, W. A. 1984, Discrete-ordinates solutions of the radiative transport equation for rectangular enclosures, Journal of Heat Transfer 106, 699-706

Fletcher, D., Haynes, B., Christo, F. and Joseph, S. 2000, A CFD based combustion model of an entrained flow biomass gasifier, Applied Mathematical Modelling 24, 165-182

Fluent Inc, 2012. Fluent 14.5 User's Guide

Galletti, C., Parente, A. and Tognotti, L. 2008, CFD simulations of MILD combustion, 8th European Conference on Industrial Furnaces and Boilers, Vilamoura, Portugal

Ganesan, V., Kumar, J. S. and Balasubramanian, V. 2004, Flow field analysis of a multi cylinder SI engine air intake system using CFD, SAE Technical Paper -, 2004-28-0010

Ghamari, M. M. S. and Nasiritosi, A. 2003, Intake manifold optimization by using 3-D CFD analysis, SAE Technical Paper -, 2003-32-0073.

Hairuddin, A. A., Wandel, A. P. and Yusaf, T. 2011, Predicting the combustion behaviour of a diesel HCCI engine using a zero-dimensional single-zone model, Australian Combustion Symposium (ACS), Newcastle, Australia.

Hanjalic, K. 1999, Second-moment turbulence closures for CFD: needs and prospects, International Journal of Computational Fluid Dynamics 12(1), 67-97.

Hasegawa, T., Mochida, S. and Gupta, A.K. 2002 Development of advanced industrial furnace using highly preheated air combustion, Journal of Propulsion and Power, 18(2): 233-239.

Hekkens, R. H. 2004, Isothermal CFD model of the HEC burner and furnace, Technical Report G108/y/1, IFRF Research Station.

Hottel, H. C. and Sarofim, A. F. 1967, Radiative transfer, McGraw-Hill, New York

IEA. 2009. World energy outlook. Paris, International Energy Agency

Joannon, D.M., Sabia, P., Sorrentino, G. and Cavaliere, A. 2009 Numerical study of MILD combustion in hot diluted diffusion ignition (HDDI) regime, Proceedings of the Combustion Institute, 32(2); 3147-3154.

Jones W.P. and Launder B.E. (1972), The Prediction of Laminarization with a Two Equation Model of Turbulence, International Journal of Heat and Mass Transfer 15, 301-314.

Katsuki, M. and Hasegawa, T. 1998 The science and technology of combustion in highly preheated air. Proceedings of the Combustion Institute, 27(2): 3135-3146

Kee, R. J., Rupley, F. M. and Miller, J. A. 1989, CHEMKIN-II: A Fortran chemical kinetics package for the analysis of gas-phase chemical kinetics, Technical Report No. SAND 89-8009B, Sandia National Laboratories, Livermore, CA

Keramiotis, C. and Founti, M.A. 2013. An experimental investigation of stability and operation of a biogas fuelled porous burner, Fuel 103:278-284.

Khoshhal, A., Rahimi, M. and Alsaira, A. A. 2009, CFD Investigation on the effect of air temperature on air blowing cooling system for preventing tube rupture, International Communication of Heat and Mass Transfer 36, 750-756.

Khoshhal, A., Rahimi, M. and Alsaira, A. A. 2010, The CFD modelling of NOx emission HiTAC and heat transfer in an industrial boiler, Numerical Heat Transfer A 58, 295-312.

Khoshhal, A., Rahimi, M., Ghahramani, A. and Alsaira, A. A. 2011, CFD modelling of high temperature air combustion in an heat recovery steam generator boiler, Korean Journal of Chemical Engineering 28(5), 1181-1187.

Kong, S. C. and Reitz, R. D. 2002 Application of detailed chemistry and CFD for predicting direct injection HCCI engine combustion and emissions, Proceedings of the Combustion Institute 29, 663-669.

Lam, S. Y., Shuaib, N. H., Hasini, H. and Shuaib, N. A. 2012, Computational fluid dynamics investigation on the use of heat shield for Thermal management in car underhood, Int. Journal of Automotive and Mechanical Engineering, 6, 785-796.

Launder BE and Sharma BI 1974 Application of the Energy Dissipation Model of Turbulence to the Calculation of Flow Near a Spinning Disc, Letters in Heat and Mass Transfer, 1(2), 131-138.

Launder, B.E. and Spalding, D.B. 1974. The numerical computation of turbulent flows, Computer Methods in Applied Mechanics and Engineering 3 (2): 269–289.

Li B W, Chen H G, Zhou J H, Cao X Y, and Cen K F, 2002 The spherical surface symmetrical equal dividing angular quadrature scheme for discrete ordinates Method, ASME Journal Heat Transfer, 124, 482-490

Li P.F., Mi J., Dally, B.B., Craig, R.A. and Wang, P. F. 2011a. Premixed moderate or intense low-oxygen dilution (MILD) combustion from a single jet burner in a lab-scale furnace, Energy Fuels, 25: 2782-2793

Li, P.F., Mi, J.C., Dally, B.B., Wang, F.F., Wang, L., Liu, Z.H., Chen, S. and Zheng, C. G. 2011b. Progress and recent trend in MILD combustion, Science China Technological Sciences, 54: 255-269

Ling, J. and Tun, L. T. Y. 2006, CFD analysis of Non-symmetrical intake manifold for formula SAE car, SAE Technical Paper 2006-01-1976

Maczulak, A 2010 Renewable energy, sources and methods, New York, Facts on File Inc

Majda A. and Sethian J.A. 1985 The derivation and numerical solution of the equations for zero mach number combustion, Combust. Sci. Tech. 42, 185-205

Mancini, M. and Weber, R. 2008, CFD method and detailed mechanisms modelling in predicting NOx in MILD combustion, 7th international symposium on High Temperature Air Combustion and Gasification, Phuket, Thailand

Medwell, P.R., Kalt, P.A.M. and Dally, B.B. 2007. Simultaneous imaging of OH, formaldehyde, and temperature of turbulent nonpremixed jet flames in a heated and diluted coflow, Combustion and Flame, 148(1-2): 48-61.

Mi, J.C., Li, P.F. and Zheng, C.G. 2010. Numerical simulations of flameless premixed combustion in a recuperative furnace, Chinese Journal of Chemical Engineering, 18(1): 10-17.

Mi, J.C., Li, P.F., Dally, B.B., Wang, F.F., Wang, L., Liu, Z.H., Chen, S. and Zheng, C.G. 2009. Importance of initial momentum rate and air-fuel premixing on MILD combustion in a recuperative furnace, Energy Fuels, 23(11): 5349-5356.

Milani, A. and Wünning, J.G. 2007 Flameless oxidation technology, advanced combustion and aero thermal technologies, Environmental Protection and Pollution Reductions, 6: 343-352

Mollica, E., Giacomazzi, E. and Marco, A. D. 2010, RANS based numerical study of hydrogen MILD combustion, European Conference on CFD, Lisbon, Portugal.

Najiha, M.A., Rahman, M.M., Yusoff, A.R. and Kadirgama, K. 2012a Investigation of flow behavior in minimum quantity lubrication nozzle for end milling processes. International Journal of Automotive and Mechanical Engineering, 6, 768-776.

Najiha, M.A., Rahman, M.M., Kamal, M., Yusoff, A.R. and Kadirgama, K. 2012b Minimum quantity lubricant flow analysis in end milling processes: a computational fluid dynamics approach, Journal of Mechanical Engineering and Sciences 3, 340-345.

Nardo, A. D., Calchetti, G., Mongibello, G., Caprariis, B. and Rufoloni, M. 2009, Coal water slurry oxy-combustion CFD analysis, International Conference on Sustainable Fossil Fuels for Future Energy, Rome, Italy

Noor M.M., Wandel, A.P. and Yusaf, T. 2012a A review of MILD combustion and open furnace design consideration, International Journal of Automotive and Mechanical Engineering, 6, 730-754

Noor M.M., Wandel, A.P. and Yusaf, T. 2012b The modelling of the effect of air fuel ratio on unburned hydrocarbons for MILD combustion, 2nd Malaysian

Postgraduate Conference, 7-9 Jul, Bond University, Gold Coast, Australia, Paper No. MPC2012-27: 159-163.

Noor M.M., Wandel, A.P. and Yusaf, T. 2012c Numerical investigation of influence of air and fuel dilution for open furnace MILD combustion burner, Southern Regional Engineering Conference, Engineers Australia, 1-2 Sept, USQ, Paper No. SREC2012-002

Noor, M. M., Kadirgama, K., R, D., Sani, M.S.M., Nawi, M.F.M. and Yusaf, T.F. 2008 CFD simulation and validation of the In-cylinder within a motored two stroke SI engine, 2nd Int. Conference on Science and Technology, Applications in Industry and Education, 12-13 Dec, UiTM Penang, 1461-1468

Noor, M. M., Wandel, A. P. and Yusaf, T. F. 2012d, A preliminary study of control parameters for open furnace MILD combustion using CFD, Malaysian Postgraduate Conference, Bond University, Gold Coast, Australia, Bond University, Gold Coast, Australia, Paper ID: MPC2012-16: 46-60

Noor, M.M., Hairuddin, A.A., Wandel, A.P. and Yusaf, F. 2012e Modelling of non-premixed turbulent combustion of hydrogen using conditional moment closure method, IOP: Materials Science and Eng. 36, Paper No. 012036:1-17

Noor, M.M., Wandel, A.P. and Yusaf, F. 2012f, The study of air fuel ratio for MILD combustion of biogas on bluff-body burner, Southern Regional Engineering Conference, Engineers Australia', USQ, Australia, Paper ID: SREC2012-01.

Noor, M.M., Wandel, A.P. and Yusaf, T. 2013, The analysis of recirculation zone and ignition position of non-premixed bluff-body for biogas MILD combustion, 2nd Int. Conference of Mechanical Engineering Research. 1-3 Jul, Malaysia, Paper No.: ICMER2013-P245.

Oryani, H., Khalilarya, S., Jafarmadar, S., Khatamnezhad, H. and Majidyfar, S. 2011 Numerical investigation of influence of dilution in air and fuel sides on MILD combustion burner. Australian Journal of Basic and Applied Science, 5(10): 272-279.

Peters, N. 2004 Turbulent combustion, Cambridge University Press

Pomeroy, C.A. 2008 Science watch-biogas breakthrough, The Japan Journal, November, 1-3

Porcheron, L., Ferrand, L., Masson, E., Aguil, F., Quinqueneau, A., Honor, D. and Boukhalfa, A. 2005, High temperature air combustion burner: semi-industrial scale experiment and CFD simulation, 6th International Symposium on High Temperature Air Combustion and Gasification, Essen, Germany.

Press, W. H., Teukolsky, S. A., Vetterling, W. T. and Flannery, B. P. 1992, Numerical recipes in fortran, Cambridge University Press.

Rahimi, M., Khoshhal, A. and Shariati, S. M. 2006, CFD modelling of a boilers Tubes rupture, Applied Thermal Engineering 26, 2192-2200

Ramasamy, D., Noor, M.M., Kadirgama, K., Mahendran, S., Redzuan, A., Sharifian, S. A. and Buttsworth, D. R. 2009 Validation of drag estimation on a vehicle body using CFD, International Association of Science and Technology for Development, Europe Power And Energy Systems, Sept, Spain.

Rebola, A., Coelho, P. J. and Costa, M. 2010 Assessment of the performance of Several turbulence and combustion models in the numerical simulation of MILD combustion in a laboratory combustor, European Conference on Computational Fluid Dynamics, 14-17 Jun, Lisbon, Portugal.

Rehm R. and Baum H. 1978 The equation of motion for thermally driven bouyant flows, N. B. S. J. Res, 83, 297-308

Salunkhe, D.B., Rai, R.K. and Borkar, R.P. 2012 Biogas technology, International Journal of Engineering Science and Technology 4(12), 4934-4940

Scholz, V. and Ellner, J. 2011 Use of biogas in fuel cells - current R&D, Journal of Sustainable Energy & Environment Special Issue, 11-15

Shafiee S and Topal E. 2009 When will fossil fuel reserves be diminished, Energy Policy, 37(1):181-189.

Sheng, C., Moghtaderi, B., Gupta, R. and Wall, T. F. 2004 A computational fluid dynamics based study of the combustion characteristics of coal blends in pulverised coal-fired furnace, Fuel 83(11-12), 1543-1552.

Shih, T.H., Liou, W.W. Shabbir, A, Yang, Z. and Zhu J. 1995 A new k−ε eddy-viscosity model for high Reynolds number turbulent flows-model development and validation, Computers and Fluids 24(3):227–238.

Siqueura, C. d. L. R., Kessler, M. P., Araujo, L.A.R.D. and Rodrigues, E.C. 2006 Three dimensional transient simulation of an intake manifold using CFD Techniques, SAE Technical Paper 2006-01-2633.

Smith, T. F., Shen, Z. F. and Friedman, J. N. 1982 Evaluation of coefficients for the weighted sum of gray gases model, ASME Journal Heat Transfer, 104, 602-608

Soufiani A and Djavdan E, 1994 A comparison between weighted sum of gray gases and statistical narrow-band radiation models for combustion applications, Combustion and Flame, 97, 240-250

Stefanidis, G. D., Merci, B., Heynderickx, G. J. and Marin, G. B. 2006 CFD simulations of steam cracking furnaces using detailed combustion mechanisms, Computers and Chemical Engineering 30, 635-649.

Szego, G. G., Dally, B. B. and Christo, F. C. 2009, Investigation of the mixing patterns inside a MILD combustion furnace based on CFD modelling, Australia Combustion Symposium, University of Newcastle, Australia. Paper ID: 2009-28.

Szego, G. G., Dally, B. B., Nathan, G. J. and Christo, F. C. 2003, Design optimisation of a MILD combustion furnace based on CFD modelling, Australia Combustion Symposium and the 8th Aust. Flame Days, Monash University, Paper ID: P047

Tsuji, H., Gupta, A., Hasegawa, T., Katsuki, M., Kishimoto, K. and Morita, M. 2003 High temperature air combustion, from energy conservation to pollution reduction, Boca Raton, FL, CRC Press

Wandel, A.P. 2005 Development of multiple mapping conditioning (MMC) for application to turbulent combustion, PhD thesis, Division of Mechanical Engineering, The University of Queensland

Wandel, A.P. 2011 A Stochastic micro mixing model based on the turbulent diffusion length scale, Australia Combustion Symposium (ACS), University of Newcastle, Australia. Paper ID: ACS2011-20.

Wandel, A.P. 2012 Extinction precursors in turbulent sprays, International Symposium on Combustion, Warsaw University of Technology, Poland, Paper ID: 1B11

Wandel, A.P., Smith, N. S. A. and Klimenko, A. Y. 2003 Implementation of multiple mapping conditioning for single conserved scalar, Second International Conference on CFD, Springer-Verlag, 789-790.

William, S. D. and McCracken, D. D. 1972, Numerical methods with Fortran IV case studies, John Wiley & Sons, New York

Wünning, J. 1991 Flammenlose oxidation von Brennstoff mit hochvorgewärmter Luft, Chemie Ingenieur Technik, 63(12): 1243-1245.

Wünning, J.A. and Wünning, J.G. 1997. Flameless oxidation to reduce thermal no-formation, Progress in Energy and Combustion Science, 23(1): 81-94.

Wünning, J.G. 1996. Flammlose oxidation von Brennstoff. PhD Thesis, University of Technology, Aachen

Yang, W. and Blasiak, W. 2006 CFD as applied to high temperature air combustion in industrial furnaces, IFRF Industrial Combustion Journal 200603

Yeoh G H and Yeun K K 2009 Computation fluid dynamics in fire engineering, Elsevier Publishing Company

Yimer, I., Becker, H. A. and Grandmaison, E. W. 2001 The strong jet/weak-Jet problem: new experiments and CFD, Combustion and Flame 124, 481-502.

Yusaf, T., Noor, M.M. and Wandel, A.P. 2013, MILD combustion: the future for lean and clean combustion, 2nd International Conference of Mechanical Engineering Research. 1-3 Jul, Malaysia, Paper No.: ICMER2013-K01.

Appendix A

Main screen on Solution Setup

Meshing
  Mesh Generation
Solution Setup
  General
  Models   **Models** (Solution Setup)
  Material   Multiphase – Off
  Phases   Energy – On
  Cell Zone Condition   Viscous – Realization k-epsilon,
  Boundary Condition   Standard Wall Fn
  Mesh Interfaces   Radiation - Discrete Ordinates (DO)
  Dynamic Mesh   Heat Exchanger - Off
  Reference Values   Species – Non-Premixed Combustion
Solution   Inert - Off
  Solution Methods NO_x - On
  Solution Controls SO_x - Off
  Monitors   Soot – Off
  Solutions Initialization   Decoupled Detailed Chem. - Off
  Calculation Activities   Reacting Channel Model - Off
  Run Calculation   Discrete Phase - Off
Result   Solidification & Melting - Off
  Graphics and Animations   Acoustics - Off
  Plots   Eulerian Wall Film - Off
  Reports